Engineering the optical response of plasmonic nanoantennas

Holger Fischer and Olivier J. F. Martin

Nanophotonics and Metrology Laboratory, Swiss Federal Institute of Technology Lausanne (EPFL), 1015 Lausanne, Switzerland

holger.fischer@epfl.ch

nam.epfl.ch

Abstract: The optical properties of plasmonic dipole and bowtie nanoantennas are investigated in detail using the Green's tensor technique. The influence of the geometrical parameters (antenna length, gap dimension and bow angle) on the antenna field enhancement and spectral response is discussed. Dipole and bowtie antennas confine the field in a volume well below the diffraction limit, defined by the gap dimensions. The dipole antenna produces a stronger field enhancement than the bowtie antenna for all investigated antenna geometries. This enhancement can reach three orders of magnitude for the smallest examined gap. Whereas the dipole antenna is monomode in the considered spectral range, the bowtie antenna exhibits multiple resonances. Furthermore, the sensitivity of the antennas to index changes of the environment and of the substrate is investigated in detail for biosensing applications; the bowtie antennas show slightly higher sensitivity than the dipole antenna.

OCIS codes: (240.6680) Surface plasmons; (260.3910) Metal optics; (310.6628) Subwavelength structures, nanostructures; (140.4780) Optical resonators; (260.5740) Resonance.

References and links

1. W. Gotschy, K. Vonmetz, A. Leitner, and F. R. Aussenegg, "Optical dichroism of lithographically designed silver nanoparticle films," Opt. Lett. **21**, 1099 (1996).
2. S. J. Oldenburg, R. D. Averitt, S. L. Westcott, and N. J. Halas, "Nanoengineering of optical resonances," Chem. Phys. Lett. **288**, 243-247 (1998).
3. J. Kottmann, O. Martin, D. Smith, and S. Schultz, "Spectral response of plasmon resonant nanoparticles with a non-regular shape," Optics Express **6**, 213-219 (2000).
4. H. Ditlbacher, B. Lamprecht, A. Leitner, and F. R. Aussenegg, "Spectrally coded optical data storage by metal nanoparticles," Opt. Lett. **25**, 563-565 (2000).
5. H. Tamaru, H. Kuwata, H. T. Miyazaki, and K. Miyano, "Resonant light scattering from individual Ag nanoparticles and particle pairs," Appl. Phys. Lett. **80**, 1826-1828 (2002).
6. G. Schider, J. R. Krenn, A. Hohenau, H. Ditlbacher, A. Leitner, F. R. Aussenegg, W. L. Schaich, I. Puscasu, B. Monacelli, and G. Boreman, "Plasmon dispersion relation of Au and Ag nanowires," Phys. Rev. B **68**, 155427 (2003).
7. J. Aizpurua, P. Hanarp, D. S. Sutherland, M. Käll, G. W. Bryant, and F. J. García de Abajo, "Optical Properties of Gold Nanorings," Phys. Rev. Lett. **90**, 057401 (2003).
8. C. L. Nehl, H. Liao, and J. H. Hafner, "Optical Properties of Star-Shaped Gold Nanoparticles," Nano Lett. **6**, 683-688 (2006).
9. L. J. Sherry, R. Jin, C. A. Mirkin, G. C. Schatz, and R. P. VanDuyne, "Localized Surface Plasmon Resonance Spectroscopy of Single Silver Triangular Nanoprisms," Nano Lett. **6**, 2060-2065 (2006).
10. H. Wang, D. W. Brandl, F. Le, P. Nordlander, and N. J. Halas, "Nanorice: A Hybrid Plasmonic Nanostructure," Nano Lett. **6**, 827-832 (2006).

#93493 - $15.00 USD Received 7 Mar 2008; revised 25 May 2008; accepted 30 May 2008; published 5 Jun 2008

11. D. P. Fromm, A. Sundaramurthy, P. J. Schuck, G. Kino, and W. E. Moerner, "Gap-Dependent Optical Coupling of Single "Bowtie" Nanoantennas Resonant in the Visible," Nano Lett. **4**, 957-961 (2004).
12. P. Mühlschlegel, H.-J. Eisler, O. J. F. Martin, B. Hecht, and D. W. Pohl, "Resonant optical antennas," Science **308**, 1607-1608 (2005).
13. S. Nie, and S. R. Emory, "Probing Single Molecules and Single Nanoparticles by Surface-Enhanced Raman Scattering," Science **275**, 1102-1106 (1997).
14. K. Kneipp, Y. Wang, H. Kneipp, L. T. Perelman, I. Itzkan, R. R. Dasari, and M. S. Feld, "Single Molecule Detection Using Surface-Enhanced Raman Scattering (SERS)," Phys. Rev. Lett. **78**, 1667 (1997).
15. H. Xu, E. J. Bjerneld, M. Käll, and L. Brjesson, "Spectroscopy of Single Hemoglobin Molecules by Surface Enhanced Raman Scattering," Phys. Rev. Lett. **83**, 4357 (1999).
16. N. Felidj, J. Aubard, G. Levi, J. R. Krenn, A. Hohenau, G. Schider, A. Leitner, and F. R. Aussenegg, "Optimized surface-enhanced Raman scattering on gold nanoparticle arrays," Appl. Phys. Lett. **82**, 3095-3097 (2003).
17. W. Zhang, X. Cui, B.-S. Yeo, T. Schmid, C. Hafner, and R. Zenobi, "Nanoscale Roughness on Metal Surfaces Can Increase Tip-Enhanced Raman Scattering by an Order of Magnitude," Nano Lett. **7**, 1401-1405 (2007).
18. L. Rogobete, F. Kaminski, M. Agio, and V. Sandoghdar, "Design of plasmonic nanoantennae for enhancing spontaneous emission," Opt. Lett. **32**, 1623-1625 (2007).
19. T. H. Taminau, F. D. Stefani, F. B. Segerink and N. F. Van Hulst, "Optical antennas direct single-molecule emission," Nature Photonics **2**, 234-237 (2008).
20. S. Kühn, U. Håkanson, L. Rogobete, and V. Sandoghdar, "Enhancement of Single-Molecule Fluorescence Using a Gold Nanoparticle as an Optical Nanoantenna," Phys. Rev. Lett. **97**, 017402 (2006).
21. T. H. Taminiau, R. J. Moerland, F. B. Segerink, L. Kuipers, and N. F. vanHulst, "$\lambda/4$ Resonance of an Optical Monopole Antenna Probed by Single Molecule Fluorescence," Nano Lett. **7**, 28-33 (2007).
22. P. Bharadwaj and L. Novotny, "Spectral dependence of single molecule fluorescence enhancement," Optics Express **15**, 14266-14274 (2007).
23. F. Tam, G. P. Goodrich, B. R. Johnson, and N. J. Halas, "Plasmonic Enhancement of Molecular Fluorescence," Nano Lett. **7**, 496-501 (2007).
24. J. N. Farahani, D. W. Pohl, H. J. Eisler, and B. Hecht, "Single Quantum Dot Coupled to a Scanning Optical Antenna: A Tunable Superemitter," Phys. Rev. Lett. **95**, 017402-017404 (2005).
25. G. Lévêque, and O. J. F. Martin, "Tunable composite nanoparticle for plasmonics," Opt. Lett. **31**, 2750-2752 (2006).
26. K. H. Su, Q. H. Wei, and X. Zhang, "Tunable and augmented plasmon resonances of Au/SiO[sub 2]/Au nanodisks," Appl. Phys. Lett. **88**, 063118-063113 (2006).
27. E. Cubukcu, E. A. Kort, K. B. Crozier, and F. Capasso, "Plasmonic laser antenna," Appl. Phys. Lett. **89**, 093120-093123 (2006).
28. J. Li, A. Salandrino, and N. Engheta, "Shaping light beams in the nanometer scale: A Yagi-Uda nanoantenna in the optical domain," Phys. Rev. B (Condensed Matter and Materials Physics) **76**, 245403-245407 (2007).
29. Z. Jiasen, and X. W. Jing Yang, and Q. Gong, "Electric field enhancing properties of the V-shaped optical resonant antennas," Optics Express **15**, 16852-16859 (2007).
30. O. L. Muskens, and J. A. S.-G. V. Giannini, and J. Gómez Rivas, "Optical scattering resonances of single and coupled dimer plasmonic nanoantennas," Optics Express **15**, 17736-17746 (2008).
31. R. M. Bakker, and Z. L. Alexandra Boltasseva, Rasmus H. Pedersen, Samuel Gresillon, Alexander V. Kildishev, Vladimir P. Drachev, and Vladimir M. Shalaev, "Near-field excitation of nanoantenna resonance," Optics Express **15**, 13682 (2007).
32. M. L. Brongersma, "Engineering optical nanoantennas," Nature Photonics **2**, 270-273 (2008).
33. A. Alu, and N. Engheta, "Tuning the scattering response of optical nanoantennas with nanocircuit loads," Nature Photonics **2**, 307-309 (2008).
34. J. Merlein, M. Kahl, A. Zuschlag, A. Sell, A Halm, J. Boneberg, P. Leiderer, A. Leitenstorfer, and R. Bratschitsch, "Nanomechanical control of an optical antenna," Nature Photonics **2**, 230-233 (2008).
35. L. Wang, S. M. Uppuluri, E. X. Jin, and X. Xu, "Nanolithography Using High Transmission Nanoscale Bowtie Apertures," Nano Lett. **6**, 361-364 (2006).
36. A. Sundaramurthy, P. J. Schuck, N. R. Conley, D. P. Fromm, G. S. Kino, and W. E. Moerner, "Toward Nanometer-Scale Optical Photolithography: Utilizing the Near-Field of Bowtie Optical Nanoantennas," Nano Lett. **6**, 355-360 (2006).
37. P. J. Schuck, D. P. Fromm, A. Sundaramurthy, G. S. Kino, and W. E. Moerner, "Improving the Mismatch between Light and Nanoscale Objects with Gold Bowtie Nanoantennas," Phys. Rev. Lett. **94**, 017402-017404 (2005).
38. O. L. Muskens, V. Giannini, J. A. Sanchez-Gil, and J. Gómez Rivas, "Strong Enhancement of the Radiative Decay Rate of Emitters by Single Plasmonic Nanoantennas," Nano Lett. **7**, 2871-2875 (2007).
39. R. M. Bakker, H.-K. Yuan, Z. Liu, V. Drachev, A. V. Kildishev, V. M. Shalaev, R. H. Pedersen, S. Gresillon, and A. Boltasseva, "Enhanced localized fluorescence in plasmonic nanoantennae," Appl. Phys. Lett. **92**, 043101 (2008).
40. O. J. F. Martin, and N. B. Piller, "Electromagnetic scattering in polarizable backgrounds," Phys. Rev. E **58**, 3909-3915 (1998).

#93493 - $15.00 USD Received 7 Mar 2008; revised 25 May 2008; accepted 30 May 2008; published 5 Jun 2008

41. M. Paulus, P. Gay-Balmaz, and O. J. F. Martin, "Accurate and efficient computation of the Green's tensor for stratified media," Phys. Rev. E**62**, 5797-5807 (2000).
42. M. Paulus, and O. J. F. Martin, "Light propagation and scattering in stratified media: a Green's tensor approach," Journal of the Optical Society of America A **18**, 854-861 (2001).
43. P. B. Johnson, and R. W. Christy, "Optical Constants of the Noble Metals," Phys. Rev. B **6**, 4370-4379 (1972).
44. J. P. Kottmann, and O. J. F. Martin, "Accurate solution of the volume integral equation for high-permittivity scatterers," IEEE Trans. Antennas Propag. **48**, 1719-1726 (2000).
45. P. Gay-Balmaz, and O. J. F. Martin, "Validity domain and limitation of non-retarded Green's tensor for electromagnetic scattering at surfaces," Opt. Comm. **184**, 37-47 (2000).
46. J. P. Kottmann, O. J. F. Martin, D. R. Smith, and S. Schultz, "Plasmon resonances of silver nanowires with a nonregular cross section," Phys. Rev. B **64**, 235402/235401-235410 (2001).
47. J. P. Kottmann, and O. J. F. Martin, "Plasmon resonant coupling in metallic nanowires," Optics Express. **4** June 2001; 8(12): (2001).
48. W. Rechberger, A. Hohenau, A. Leitner, J. R. Krenn, B. Lamprecht, and F. R. Aussenegg, "Optical properties of two interacting gold nanoparticles," Opt. Comm. **220**, 137-141 (2003).
49. C. A. Balanis, Antenna Theory: Analysis and Design (Wiley-Interscience, Hoboken, NJ, 2005).
50. L. Novotny, "Effective Wavelength Scaling for Optical Antennas," Phys. Rev. Lett. **98**, 266802-266804 (2007).

1. Introduction

Over the last 10 years there has been a surge of research in the optical properties of metallic nanoparticles [1–10]. Properly designed nanostructures are known to produce so called hot spots where the incident electromagnetic field is enhanced by several orders of magnitude. The plasmonic resonances observed in such structures open the possibility to build antennas operating in the visible [11,12]. Their hot spots can be used to trigger nonlinear effects and to couple electromagnetic radiation efficiently between the antennas and dipole emitters. Experimental techniques such as tip enhanced Raman spectroscopy or surface enhanced Raman spectroscopy demonstrate the potential of such hot spots to detect radiative emitters with sensitivity down to a single molecule [13–19]. The enhancement of the fluorescence of molecules placed near a plasmonic nanostructure has been observed recently, tuning the plasmon resonance either to the excitation or the emission of the molecules [20–23].

The optical properties of different types of antennas have been discussed over the last few years [24–34]. Two geometries, i.e. the dipole and the bowtie antennas, appear to combine in a unique way the formation of a strong hot spot in their gap and the tunability of their resonance. The strong field enhancement of dipole antennas has readily been shown by white light continuum generation [12]. Bowtie antennas have recently been used as near-field probes

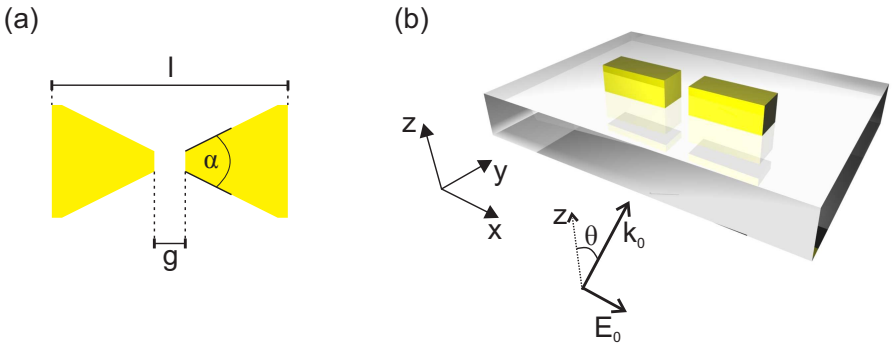

Fig. 1. Geometry of the investigated system: (a) Bowtie and (b) dipole antennas. The illumination is shown in panel (b).

#93493 - $15.00 USD Received 7 Mar 2008; revised 25 May 2008; accepted 30 May 2008; published 5 Jun 2008

and for nanolithography [35, 36]. The potential of both structures for the enhancement of the fluorescence of molecules has also been demonstrated [37–39]. However a detailed analysis and comparison of the optical properties of both antenna structures as a function of their different geometrical parameters is still lacking in the literature. The aim of this paper is to provide such a detailed analysis.

The paper is organized as follows: Section 2 describes the model used; the response of dipole and bowtie antennas is discussed in Section 3 and a conclusion is presented in the last section.

2. Method and geometry

The Green's tensor method is used to calculate the optical response of gold dipole and bowtie antennas [40–42]. The real and imaginary parts of the gold dielectric function are obtained from experimental data [43]. To account for a realistic environment the antennas are supported by a substrate with index of refraction n_s and covered with a material with index n_{env}. It is essential to consider such environment material for applications in biosensing, where the antenna might be immersed in water or another liquid. If not specified otherwise the calculations are performed for a substrate index $n_s = 1.5$ and an environment index $n_{env} = 1.0$. The structures are illuminated from below through the substrate, perpendicular to the antenna long axis and at an angle of incidence $\theta = 70^\circ$ to the vertical axis, to fulfill the attenuated total reflection condition at the glass/air interface, as illustrated in Fig. 1(b). The incident field E_0 is polarized along the long axis of the antenna. As pointed out in the introduction, the gap represents an essential feature of the antenna structure. To characterize the spectral response of the antenna and its intensity enhancement we therefore calculate the field intensity inside this gap in relative units to the illumination intensity I_0 in the substrate. The antennas are discretized with 10x10x10nm^3 meshes, which leads to the following bow angles α for the bowtie antenna: $\alpha_1 = 28^\circ$, $\alpha_2 = 53^\circ$, $\alpha_3 = 90^\circ$ and $\alpha_4 = 127^\circ$, Fig. 1(a). All antennas have a 40nm thickness. The width of the dipole antenna is 40nm, whereas the bowtie antenna apex width is 20nm. These values correspond to what can

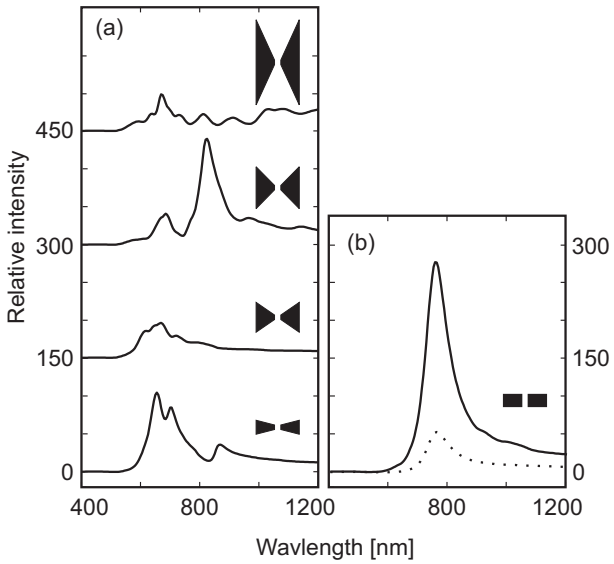

Fig. 2. Relative field intensity spectra in the gap for (a) bowtie and (b) dipole antennas. The dotted line in panel (b) indicates the relative field intensity at the extremity of the dipole antenna. (l=230nm; g=30nm)

#93493 - $15.00 USD Received 7 Mar 2008; revised 25 May 2008; accepted 30 May 2008; published 5 Jun 2008

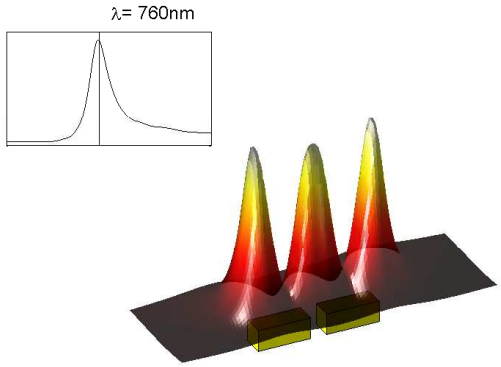

Fig. 3. Near-field intensity distribution 20nm above a dipole antenna (l=230nm) as a function of the illumination wavelength λ. The corresponding spectrum (field intensity in the gap) is shown in the inset. (file size: 0.4MB)

be achieved with modern fabrication techniques. The mesh used for the calculation provides an accurate description of the antennas; the interested reader is referred to Refs. [44, 45] for discussion of the convergence of the method and to Ref. [46] - especially Fig. 11 - for a discussion of surface roughness and local field enhancement.

In the next section, we study the spectra of dipole and bowtie antennas as a function of the following geometrical parameters: Antenna length l, gap width g, substrate index n_s and environment index n_{env}, Fig. 1(b).

3. Results and discussion

The geometry of the antenna strongly influences its optical properties as indicated in Figure 2, which shows the calculated intensity spectra in the antenna gap for the dipole antenna and for the bowtie antennas with the bow angles α_1 - α_4. In the spectral range of the calculation, the dipole antenna has one resonance at 760nm, where the field intensity in the gap is about 280 times larger than the intensity of the illumination field. The bowtie antennas produce a lower field in their gaps (about 50-150 times the illumination field intensity). Figure 2 indicates that the dipole antenna is essentially single mode, while the bowtie antennas exhibit several resonances, whose spectral positions depend on the bow angle α. However, a clear trend between bow angle and field enhancement in the bowtie antennas cannot be observed. At the smallest bow angle α_1, where the bowtie antenna resembles most the dipole antenna, its spectrum approaches most the spectrum of the dipole antenna. The strongest field enhancement is observed for the bow angle $\alpha_3 = 90^\circ$, Fig. 2(a).

The movies in Figs. 3 and 4 show the near-field intensity in a parallel plane 20nm above the structure as a function of the illumination wavelength. Each resonance corresponds to a specific mode in the near-field. Note that the asymmetry of the near-field along the y-axis is due to the inclined illumination. The bowtie antennas seem to provide a better localization of the field inside the gap, with less field enhancement at the external edges than observed for the dipole structure. However, the field intensity inside the gap of the dipole structure is larger than for the bowtie structures, as can also be seen from the spectra in Fig. 2. The dotted line in Fig. 2(b) represents the intensity at the external edges of the dipole antenna. The intensity in the gap of the dipole antenna is thus about five times larger than at the edges of the antenna. To illustrate

#93493 - $15.00 USD Received 7 Mar 2008; revised 25 May 2008; accepted 30 May 2008; published 5 Jun 2008

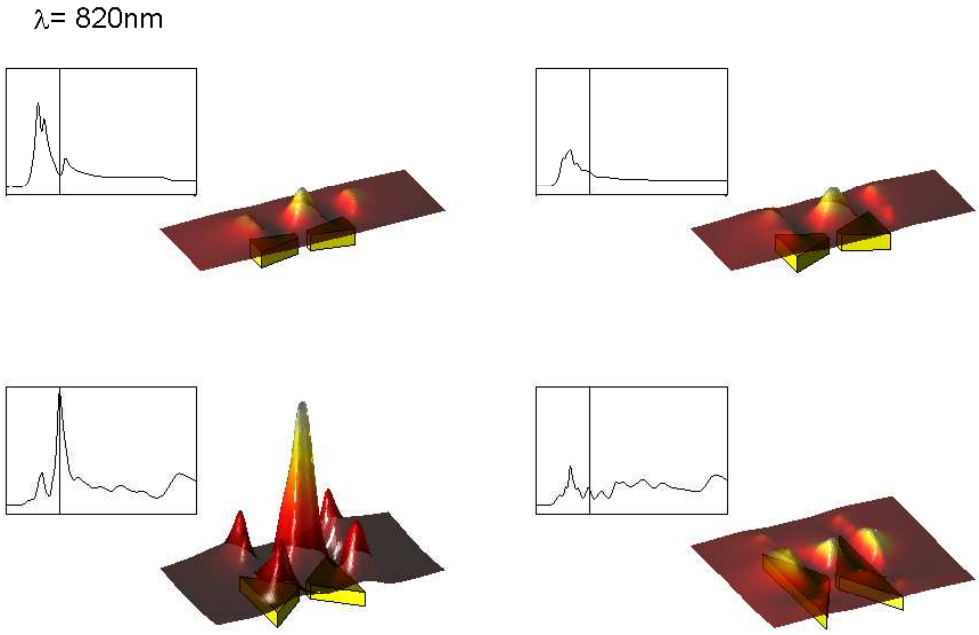

Fig. 4. Near-field intensity distributions 20nm above bowtie antennas (l=230nm) as a function of the illumination wavelength λ. Four different bow angles are considered (from top left to bottom right): $\alpha_1 = 28°$, $\alpha_1 = 53°$, $\alpha_1 = 90°$ and $\alpha_4 = 127°$. The corresponding spectra (field intensity in the gap) are shown in the insets. (file size: 1.5MB)

the strong field confinement in the antenna gap, Fig. 5 shows the field intensity in the xz- and yz-planes through the gap. The field is confined within a volume of about 40*40*30nm which is well below the limit of diffraction at a wavelength of 760nm. Note the logarithmic scale in the color-plots of Fig. 5.

The spectral positions of the antenna resonances are determined by the antenna dimensions. For the chosen incident polarization, the length of the antenna plays the most crucial role. To study this effect further and to simplify the comparison of dipole and bowtie antennas, in the

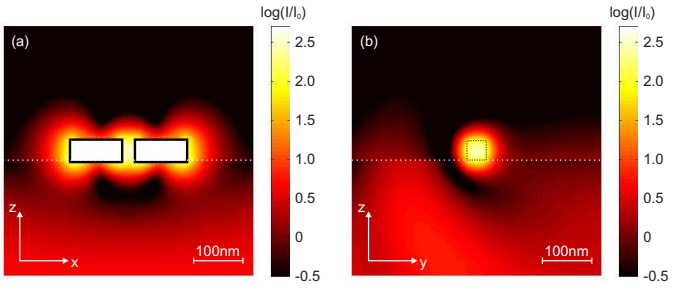

Fig. 5. (a) xz-map and (b) yz-map of the relative field intensity in a plane through the middle of a dipole antenna at the resonance wavelength.

#93493 - $15.00 USD Received 7 Mar 2008; revised 25 May 2008; accepted 30 May 2008; published 5 Jun 2008

remaining of the paper we will concentrate on the bowtie structure with a bow angle $\alpha_3 = 90^\circ$, which produces the largest field enhancement. The influence of the antenna length on the resonance spectrum is investigated in Fig. 6. Note the different intensity scales of the dipole and bowtie antennas, as well as the different intensity scales for the short (l=110nm and l=130nm) and for the long antennas, Figs. 6(a) and (b). Two resonances are observed for the short dipole antennas. In that case, the geometry resembles more that of two coupled nanoparticles, supporting two plasmon modes [47]. The low energy mode shifts very rapidly to the infrared when the structure length increases.

Longer dipole antennas ($l \geq 150$nm) exhibit one strong resonance which slightly red shifts when the antenna length increases. This effect is investigated in detail in Fig. 7(a), which shows the spectral position of the resonance as a function of the antenna length. For the dipole antenna, the resonance shifts linearly with the antenna length, with a proportion of 2.1 [wavelength/antenna length]. This trend is less obvious for the bowtie antenna, Fig 6(b). While very short antennas show again two peaks, longer bowtie antennas clearly exhibit a multimode behavior with several peaks. Tracking the resonance wavelength of the strongest mode leads to the scattered data in Fig. 7(a). However, by analyzing each resonance individually, one can recover a well defined trend, as indicated in Fig. 8. The three main resonances identified in Fig. 8(a) for an antenna length of l=210nm shift almost linearly with the antenna length, Fig 8(b). The coefficients (between 1.8 and 2.5 [wavelength/antenna length], depending on the resonance Fig. 8(b)) are comparable to that of the dipole antenna.

Figure 7(b) shows the relative field enhancement in the gap as a function of the antenna length. Both antenna types clearly exhibit a linear increase of the field intensity for the range of calculated lengths. The physical origin for this effect is connected to the coupling strength of the two antenna arms. As a matter of fact, the resonance wavelength of a long antenna is

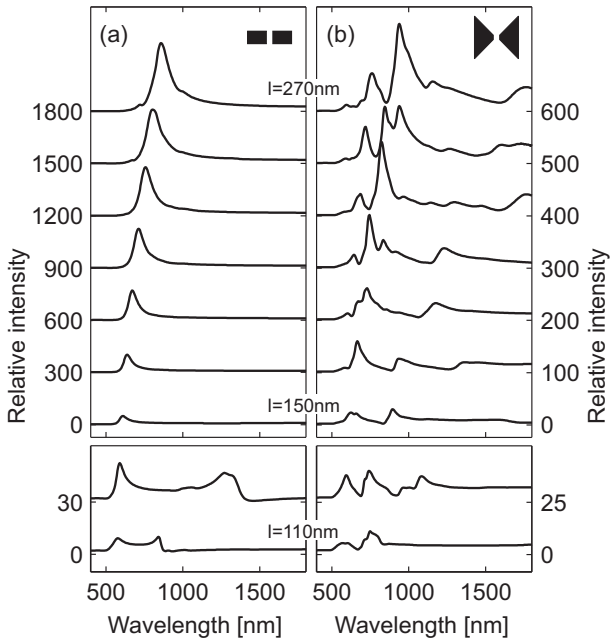

Fig. 6. Relative intensity enhancement in the gap as a function of the antenna length l between l=110nm and l=270nm in 20nm increments. (a) Dipole and (b) bowtie geometry ($\alpha = 90^\circ$). The antenna gap is kept constant (g=30nm).

#93493 - $15.00 USD Received 7 Mar 2008; revised 25 May 2008; accepted 30 May 2008; published 5 Jun 2008

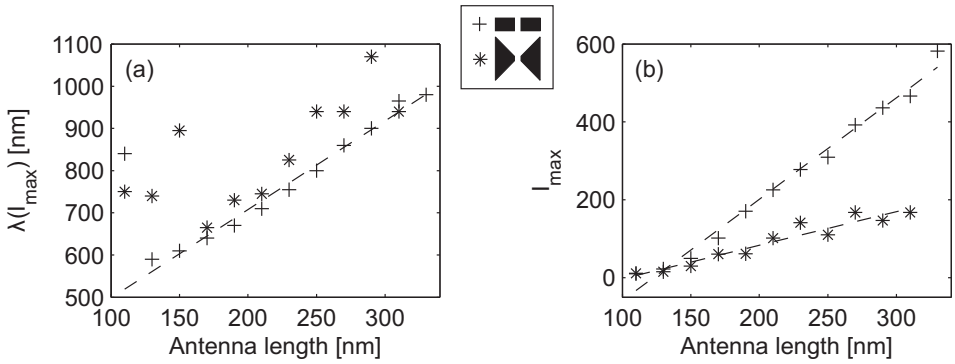

Fig. 7. (a) Resonance position shift for dipole (+) and bowtie ($\alpha = 90°$, *) antennas as a function of the antenna length. (b) Field enhancement as a function of the antenna length for both antennas.

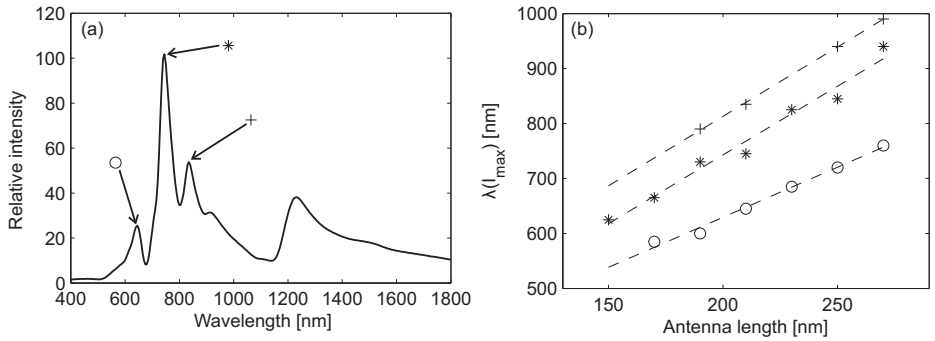

Fig. 8. (a) The three main resonances of a bowtie antenna (l=210nm;$\alpha = 90°$) and (b) their spectral position as a function of the antenna length.

larger than that of a short antenna. Hence, the gap has a smaller effective length for the larger antenna, which results in a stronger coupling between both arms. Note also in Fig. 7(b) that the increase of the field as a function of the antenna length is much stronger for the dipole antenna. However, the increment of the field in the gap of the dipole antenna is much stronger than that of the bowtie antenna. For the shortest antenna length (110nm) the field is about the same for both structures, whereas for the longest antenna (300nm) the dipole enhancement is about three times higher than the bowtie enhancement.

Stronger field enhancements can be achieved by decreasing the width of the gap. The resulting spectral response is calculated in Figs. 9(a) and (b). Note the logarithmic intensity scale for the color plots. The spectral position of the dipole resonance and of the three main bowtie resonances as a function of the gap width is shown in Fig. 9(c). For decreasing gap widths the dipole resonance shifts to the red just as observed experimentally for nanodiscs by Rechberger et al. [48]. On the other hand, the spectral position of the bowtie main resonance remains rather constant. Both dipole and bowtie antennas exhibit a strong increase of the field inside the gap for decreasing gap width, as shown in Fig. 9(d). Again this effect is much stronger for the dipole antenna than for the bowtie antenna.

Another interesting effect is visible in Fig. 9(c): For decreasing gap width, the resonance wavelength of the dipole antenna shifts towards that of a monopole antenna with the corre-

#93493 - $15.00 USD Received 7 Mar 2008; revised 25 May 2008; accepted 30 May 2008; published 5 Jun 2008

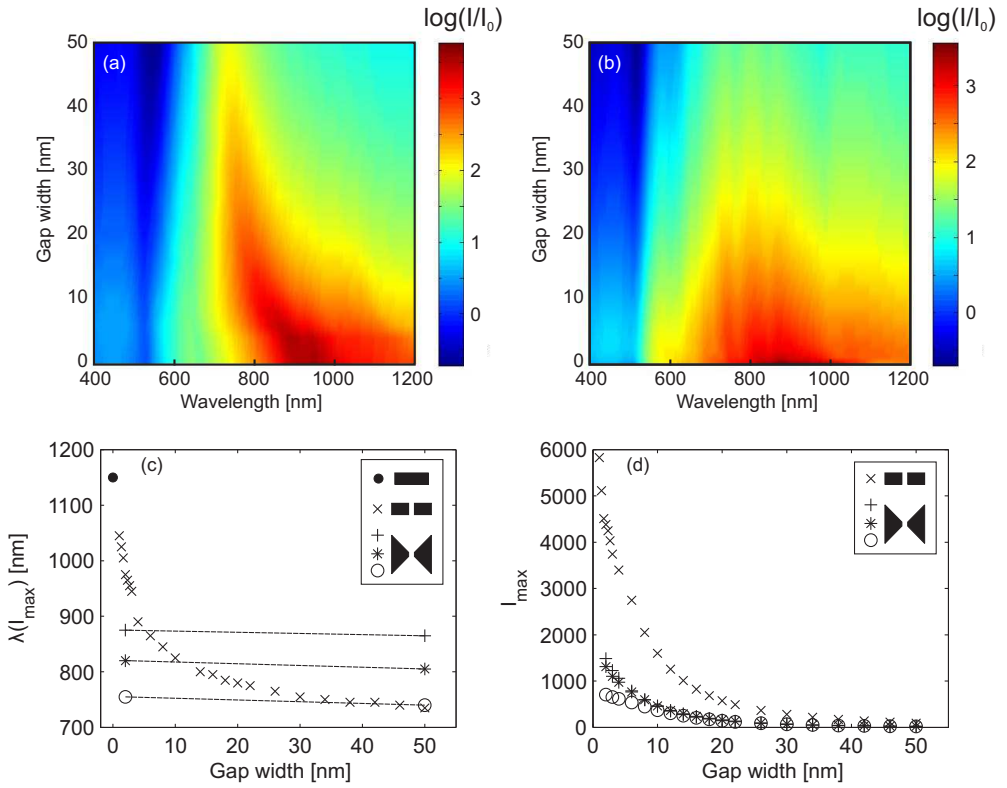

Fig. 9. Relative intensity spectra in the gap as a function of the illumination wavelength and gap width for (a) a dipole and (b) a bowtie ($\alpha = 90^\circ$) antenna (l=230nm). (c) Spectral position and (d) relative field enhancement in the gap of the corresponding intensity maximum as a function of the gap width. For the bowtie antenna the three main resonances are again treated separately (see Fig. 8). The dot in panel (c) indicates the spectral position of the maximum for the corresponding monopole antenna.

sponding length (l=200nm) indicated by a dot in Fig. 9(c). This effect is not observed for the bowtie antenna. This is probably because in the case of the bowtie geometry, the structure for touching arms (g=0) is not similar to one individual arm, as is the case for a dipole antenna. Overall, the spectrum of the bowtie antenna appears to be more determined by the resonance of the the two triangular arms, rather than by the coupling between them.

At microwave or radio frequencies, the substrate index n_s has a strong influence on the resonance spectrum of the antenna [49]. This dependence is in general used to design small antennas with dimensions well below the half wavelength condition. The same effect can be observed in Fig. 10 for optical resonant antennas: An increasing substrate index leads to a red shift of the antenna resonance. At optical frequencies the antenna dimensions are as small as a few tens of nanometers, i.e. below the half wavelength condition [50] and at the limit of today's fabrication techniques. Hence designing smaller antennas by using high index materials as substrate does not seem to be of great practical interest presently.

Much more interesting is the antenna sensitivity to changes of the environmental index of refraction n_{env}. As shown in Fig. 11 the spectral positions of the dipole and the bowtie resonances strongly depend on n_{env}. Figure 12(a) and (b) show a linear increase of the resonance wavelength for increasing n_{env}. Furthermore, the sensitivity of the dipole antenna strongly depends

#93493 - $15.00 USD Received 7 Mar 2008; revised 25 May 2008; accepted 30 May 2008; published 5 Jun 2008

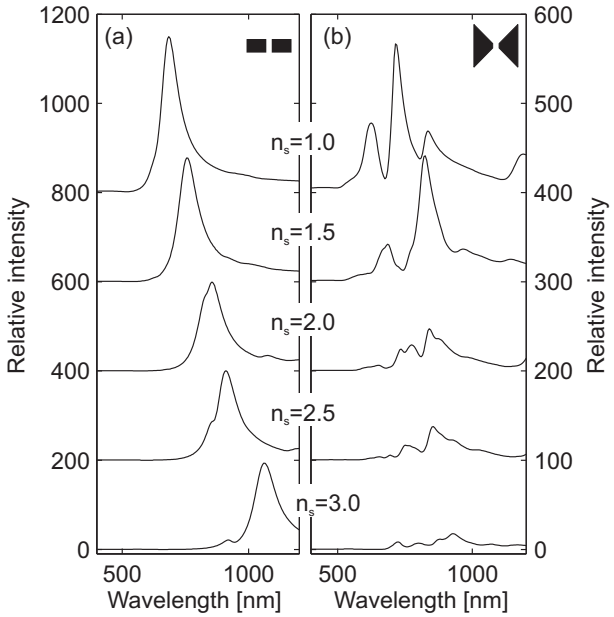

Fig. 10. Relative field intensity enhancement in the gap for (a) a dipole and (b) a bowtie antenna (l=110nm, g=30nm, $\alpha = 90^{\circ}$) as a function of the illumination wavelength. Different refractive indexes n_s are used for the substrate material.

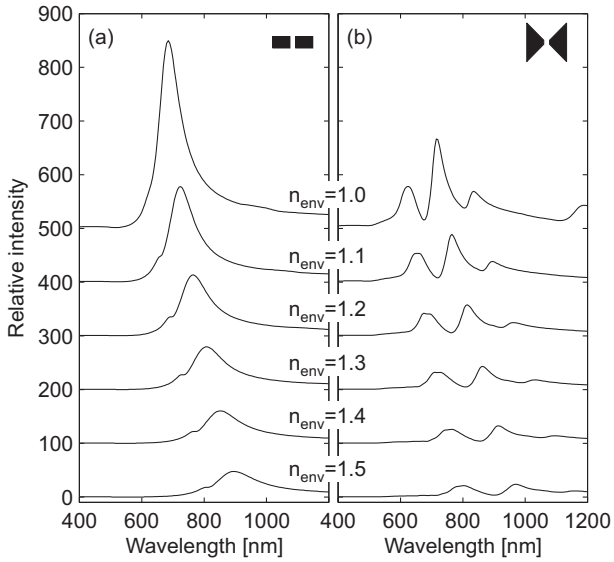

Fig. 11. Relative field intensity enhancement in the gap for (a) a dipole and (b) a bowtie antenna (l=110nm, g=30nm, $\alpha = 90^{\circ}$) as a function of the illumination wavelength. Different refractive indexes n_{env} are used for the cover material, the substrate index is n_s=1,5.

#93493 - $15.00 USD Received 7 Mar 2008; revised 25 May 2008; accepted 30 May 2008; published 5 Jun 2008

on its gap width: Decreasing the gap width increases the antenna sensitivity as shown in Fig. 12(a). For the bowtie antenna this dependence cannot be observed, Fig. 12(b). All investigated bowtie antennas show a slightly higher sensitivity than the dipole antenna (500-510RIU^{-1} vs. 400-490RIU^{-1}). We assume that this sensitivity is related to the spectral position of the antenna resonance. The further the resonance wavelength is shifted to the red, the higher the antenna sensitivity on index changes. Since we have shown previously that the resonance position of the bowtie antenna remains constant for changing gap widths, the sensitivity to the environment is not changing either for different gaps.

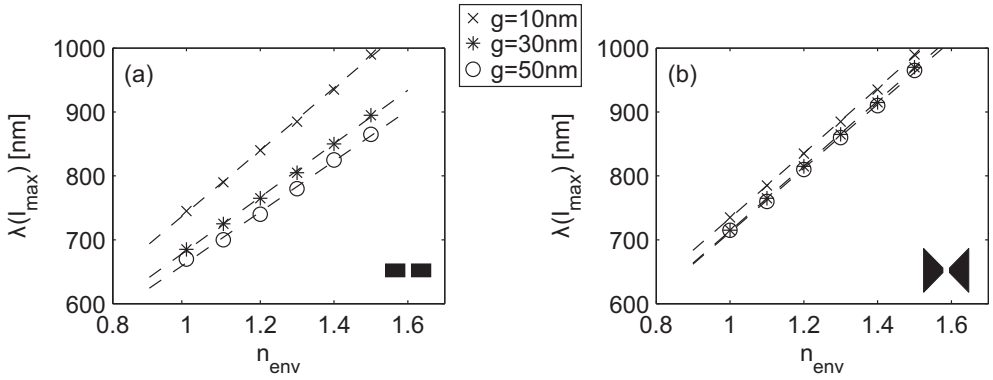

Fig. 12. Sensitivity of the (a) dipole and (b) bowtie antenna (l=110nm, g=30nm, $\alpha = 90^{\circ}$) as a function of the environment index n_{env}.

4. Conclusion

We have investigated numerically the optical properties of plasmonic dipole and bowtie nanoantennas with different bow angles as a function of the antenna length, gap, substrate and background indexes. The bowtie antenna supports multiple resonances in the examined spectral range, leading to a rather broadband response. The three main resonances appear to be very sensitive to changes in the antenna geometry. Bowtie and dipole antennas turn out to have similar tuning capabilities with their length. However, the spectral position of the dipole resonance depends much stronger on the gap width than it is the case for the bowtie antenna, where almost no spectral shift could be observed. Interestingly the field enhancement is much stronger for the dipole than for the bowtie antenna. Even though the calculated bowtie structures have a sharper tip (20nm) than the calculated dipole structures (40nm), the intensity enhancement in the dipole gap reaches values that are three times higher than that of the bowtie antenna. Despite the stronger field enhancement of the dipole antenna, the bowtie structures show stronger sensitivity to environmental index changes. To the best of our knowledge this is the first detailed comparison of the optical properties of dipole and bowtie antennas. The results of this article should be useful for choosing the best suited antenna geometry for a given application.

Acknowledgements

It is a pleasure to thank André Christ for stimulating discussions. Funding from the Swiss National Science Fundation under grants 200020-113458 and NCCR Nanoscale Science is gratefully acknowledged.

#93493 - $15.00 USD Received 7 Mar 2008; revised 25 May 2008; accepted 30 May 2008; published 5 Jun 2008